

Thomas-Fermi Calculations of Atoms and Matter in Magnetic Neutron Stars II: Finite Temperature Effects

A. Thorolfsson^{1,2}, Ö. E. Rögnvaldsson³, J. Yngvason^{1,4}

and

E. H. Gudmundsson^{1,5}

ABSTRACT

We present numerical calculations of the equation of state for dense matter in high magnetic fields, using a temperature dependent Thomas-Fermi theory with a magnetic field that takes all Landau levels into account. Free energies for atoms and matter are also calculated as well as profiles of the electron density as a function of distance from the atomic nucleus for representative values of the magnetic field strength, total matter density, and temperature. The Landau shell structure, which is so prominent in cold dense matter in high magnetic fields, is still clearly present at finite temperature as long as it is less than approximately one tenth of the cyclotron energy. This structure is reflected in an oscillatory behaviour of the equation of state and other thermodynamic properties of dense matter and hence also in profiles of the density and pressure as functions of depth in the surface layers of magnetic neutron stars. These oscillations are completely smoothed out by thermal effects at temperatures of the order of the cyclotron energy or higher.

Subject headings: atomic processes — dense matter — equation of state — non-zero temperatures — stars: neutron — stars: magnetic fields

1. Introduction

The temperature of a neutron star exceeds 10^{11} K at its birth in a supernova core collapse. Initially the star cools very rapidly due to a copious emission of neutrinos (and anti-neutrinos)

¹Science Institute, University of Iceland, Dunhaga 3, IS-107 Reykjavik, Iceland

²CETP, 4 avenue de Neptune, 94107 Saint-Maur, France

³Theoretical Astrophysics Center, Juliane Maries Vej 30, DK-2100 Copenhagen Ø, Denmark

⁴Institut für Theoretische Physik, University of Vienna, Austria

⁵Nordita, Blegdamsvej 17, DK-2100 Copenhagen Ø, Denmark

but once the interior temperature has become of the order of 10^9 K the cooling becomes slower although it is still dominated by neutrino emission for thousands of years. At later stages when the temperature has fallen sufficiently the emission of electromagnetic radiation from the surface becomes the dominant cooling mechanism (see e.g. Prakash et al. 1997; Pethick 1992; Nomoto & Tsuruta 1987; Umeda et al. 1994).

An important ingredient in calculations of neutron star cooling is the thermal structure of the envelope, i.e. the surface layers and the outer crust of the star. Although the envelope contains only a very small fraction of the star's mass, it controls the heat transport from the high density interior to the surface and thus determines the relationship between the surface temperature and the temperature of the stellar core, which is isothermal for sufficiently old stars. Among other things this relationship plays a crucial role in relating results of theoretical cooling calculations to observations of radiation from neutron star surfaces (see Gudmundsson et al. 1983, and references therein).

If the neutron star has a high magnetic field the properties of matter close to the surface are strongly modified by the field as compared to the zero field case, thus changing both density and temperature profiles in the envelope (see e.g. Rönigvaldsson et al. 1993 (hereafter Paper I), and references therein). The field may also have a considerable effect on the spectrum of radiation emitted from the stellar surface as well as its polarization and angular distribution (see e.g. Pavlov et al. 1995).

In order to investigate the thermal structure of neutron star envelopes one needs as physical input both the opacity as well as the equation of state of matter for the relevant temperatures and densities. The case of iron envelopes in zero magnetic field was investigated in detail by Gudmundsson et al. (1983), and more recently the thermal structure of envelopes with accreted layers of lighter elements has been investigated by Chabrier et al. (1997) and Potekhin et al. (1997). Several authors have also included the effects of strong magnetic fields to varying degrees of accuracy (e.g. Hernquist 1985; Van Riper 1988; Schaaf 1990a,b; Page 1995). The paper by Yakovlev & Kaminker (1994) gives a comprehensive review of the physical properties of neutron star envelopes with magnetic fields, including a general discussion of magnetic opacities. More recently Potekhin (1996) and Potekhin & Yakovlev (1996) have published practical expressions for electric and thermal conductivities along magnetic fields under conditions occurring in neutron stars, and Lai & Salpeter (1997) have investigated the effects of different phases of hydrogen on the properties of the atmospheres and surface emission of strongly magnetized neutron stars.

In this paper we extend our previous work on the zero temperature equation of state of dense matter in high magnetic fields (Paper I) by including the effects of temperature for all Landau levels. As before we use the pure Thomas-Fermi (TF) method for matter in a magnetic field, where by pure we mean that correction terms such as the exchange (Dirac) correction and the von Weizsäcker gradient correction are not included in the calculations. For the problem under discussion this is in fact a good approximation as emphasized by Fushiki et al. (1992), who present

a detailed treatment of magnetic TF theory and give extensive references to earlier work (see also Paper I and Lieb et al. 1994).

The paper is organized as follows. In §2 we first give a short general overview of TF theory at arbitrary temperature and then specialize the discussion to hot matter in high magnetic fields with all Landau levels taken into account. There we also discuss the range of validity of the theory and its scaling properties. Our numerical methods are described in §3, and in §4 we present the results of the calculations for the equation of state and the sound velocity of hot neutron star matter as well as isothermal density profiles of surface layers of neutron stars. As in Paper I we have chosen iron, with $Z = 26$ and $A = 56$, as our reference element in the numerical calculations, and the range of magnetic field strengths covered is from 10^{10} to 10^{13} G. Because of the scaling properties of TF theory, discussed in §2.5, this is not a serious restriction. The results presented in §4 are mainly in graphical form but for the convenience of potential users a tabulated version can be found at the website <http://www.raunvis.hi.is/~ath/TFBT>.

Some of the bulk properties of hot dense matter in a strong magnetic field have previously been investigated by other authors. Gadiyak et al. (1981) used a modified TF theory including more than one Landau level to calculate an equation of state for iron in a magnetic field of order 10^{12} G. Using the strong field version of the TF-method Constantinescu & Moruzzi (1978) studied the case of hot iron in bulk in the limit when the field is so strong that only the lowest Landau level is populated. A similar investigation was performed by Abrahams & Shapiro (1991) who also constructed a model including exchange and gradient correction to the equation of state of iron in the strong field limit.

2. The Thomas-Fermi Method

2.1. The General TF Equation

A quick road to TF theory at arbitrary temperature starts with the basic thermodynamical relationship between the particle density n and the pressure P_{el} for noninteracting electrons

$$n = P'_{\text{el}}(\mu) \quad (1)$$

where the dash denotes differentiation with respect to the chemical potential μ . For electrons that interact with each other and fixed nuclei by Coulomb forces the electron density depends on the position \mathbf{r} , and the electrostatic potential generated by K nuclei with charges eZ_i at positions \mathbf{R}_i together with the electrons is

$$\Phi_n(\mathbf{r}) = \sum_{i=1}^K \frac{eZ_i}{|\mathbf{r} - \mathbf{R}_i|} - e \int \frac{n(\mathbf{r}')}{|\mathbf{r} - \mathbf{r}'|} d^3\mathbf{r}'. \quad (2)$$

In the TF approximation it is assumed that the relation (1) holds locally, but the total electrochemical potential $\mu_{\text{TF}} \equiv \mu - e\Phi_n(\mathbf{r})$ of the electrons (called μ_{tot} in Paper I) is independent

of position. The TF equation for the density $n(\mathbf{r})$ thus becomes

$$n(\mathbf{r}) = P'_{\text{el}}(e\Phi_n(\mathbf{r}) + \mu_{\text{TF}}). \quad (3)$$

The constant μ_{TF} depends on the total number of electrons and the boundary conditions.

The nonlinear integral equation (3) for n may be combined with Poisson's equation

$$\nabla^2 \Phi_n(\mathbf{r}) = 4\pi e \left[n(\mathbf{r}) - \sum_{i=1}^K Z_i \delta(\mathbf{r} - \mathbf{R}_i) \right] \quad (4)$$

to obtain the TF differential equation for $\Psi \equiv e\Phi_n + \mu_{\text{TF}}$:

$$\nabla^2 \Psi(\mathbf{r}) = 4\pi e^2 P'_{\text{el}}(\Psi(\mathbf{r})) \quad (5)$$

for $\mathbf{r} \notin \{\mathbf{R}_1, \dots, \mathbf{R}_K\}$. To take care of the Coulomb singularities at the nuclear positions, (5) has to be supplemented by the boundary conditions

$$\lim_{\mathbf{r} \rightarrow \mathbf{R}_i} |\mathbf{r} - \mathbf{R}_i| \Psi(\mathbf{r}) = e^2 Z_i. \quad (6)$$

Moreover, the whole system is confined within a bounded region Ω , and the total number of electrons within Ω , N , is fixed. Integrating (4) over Ω we obtain by the divergence theorem

$$\int_{\partial\Omega} (\nabla \Psi) \cdot d\mathbf{S} = 4\pi e^2 \left(N - \sum_{i=1}^K Z_i \right). \quad (7)$$

In the spherically symmetric, neutral case considered in §2.4, Ω is a sphere with radius r_0 containing a single nucleus of charge $Z = N$ at the centre. Hence, the spherically symmetric Ψ satisfies

$$\left. \frac{d}{dr} \Psi(r) \right|_{r=r_0} = 0 \quad (8)$$

in this case.

Once (5), (6) and (7) (or (8)) have been solved the electronic density may be obtained from (3), i.e.

$$n(\mathbf{r}) = P'_{\text{el}}(\Psi(\mathbf{r})). \quad (9)$$

Likewise, the local pressure in the electron gas is

$$P_{\text{loc}}(\mathbf{r}) = P_{\text{el}}(\Psi(\mathbf{r})). \quad (10)$$

2.2. TF Theory as a Minimization Problem

By Legendre transformation one may pass from the pressure P_{el} to the free energy density

$$f_{\text{el}}(n) = \sup_{\mu} \{ \mu n - P_{\text{el}}(\mu) \}. \quad (11)$$

The derivative $f'_{\text{el}} = \partial f_{\text{el}}/\partial n$ is the inverse of P'_{el} , so (1) is equivalent to

$$\mu = f'_{\text{el}}(n) \quad (12)$$

and the TF equation (2) may be written as

$$f'_{\text{el}}(n(\mathbf{r})) - e\Phi_n(\mathbf{r}) = \mu_{\text{TF}}. \quad (13)$$

This again states that the total electrochemical potential is independent of the position. Equation (13) is the Euler-Lagrange equation of a minimization problem: Define the free energy functional of the interacting electron gas as

$$\mathcal{F}[n] = \int_{\Omega} f_{\text{el}}(n(\mathbf{r}))d^3\mathbf{r} - \sum_{i=1}^K e^2 Z_i \int_{\Omega} \frac{n(\mathbf{r})}{|\mathbf{r} - \mathbf{R}_i|} d^3\mathbf{r} + \frac{e^2}{2} \int_{\Omega} \int_{\Omega} \frac{n(\mathbf{r})n(\mathbf{r}')}{|\mathbf{r} - \mathbf{r}'|} d^3\mathbf{r}d^3\mathbf{r}'. \quad (14)$$

Then (13) is the variational equation for the minimization of (14) under the subsidiary condition

$$\int n(\mathbf{r})d^3\mathbf{r} = N = \text{constant}. \quad (15)$$

The μ_{TF} in (13) is the Lagrange multiplier corresponding to the subsidiary condition. It is given by

$$\mu_{\text{TF}} = \frac{\partial F(N)}{\partial N}$$

where $F(N) = \mathcal{F}[n_{\text{TF}}]$ is the free energy at the minimizing density n_{TF} , i.e., the solution to the TF equation (13).

2.3. The Electron Gas in a Magnetic Field at Nonzero Temperature

We shall now specialize the general scheme described above to the case of non-relativistic electrons in a strong, homogeneous magnetic field of strength B . For the rest of this section and in §3, we find it convenient to employ atomic units where Planck's constant \hbar , Boltzmann's constant k , the electron mass m_e and the elementary charge e are all taken to be 1 and dimensionless. This means that magnetic fields are measured in the natural unit

$$B_0 = \frac{m_e^2 e^3 c}{\hbar^3} = 2.35 \times 10^9 \text{ G},$$

lengths are measured in terms of the Bohr radius

$$a_0 = \frac{\hbar^2}{m_e e^2} = 0.529 \times 10^{-8} \text{ cm}$$

and energies in the unit

$$\frac{e^2}{a_0} = 27.2 \text{ eV}.$$

The corresponding temperature unit is

$$\frac{e^2}{a_0 k} = 3.16 \times 10^5 \text{ K}$$

and pressure is measured in

$$\frac{e^2}{a_0^4} = 8.2 \times 10^{26} \text{ dyn/cm}^2.$$

(When presenting our results in §4 we shall convert back to conventional units.)

The motion of the electrons perpendicular to the magnetic field is quantized into Landau levels with energy νB , $\nu = 0, 1, 2, \dots$. The degeneracy of the levels, per unit area, is $B/2\pi$ for $\nu = 0$ but twice as high for $\nu > 0$ due to the electron spin. Along the field the motion is one-dimensional with the density of states $D(\varepsilon) = \varepsilon^{-1/2}/(2^{1/2}\pi)$, where ε is the energy of the translational motion.

It follows that the particle density at temperature T and chemical potential μ is given by

$$\begin{aligned} n = P'_{\text{el}}(\mu; T, B) &= \frac{B}{2\pi} \frac{1}{2^{1/2}\pi} \left[\int_0^\infty \frac{\varepsilon^{-1/2}}{e^{(\varepsilon-\mu)/T} + 1} d\varepsilon + 2 \sum_{\nu=1}^\infty \int_0^\infty \frac{\varepsilon^{-1/2}}{e^{(\varepsilon+\nu B-\mu)/T} + 1} \right] \\ &= \frac{BT^{1/2}}{2^{3/2}\pi^2} \left[I_{-1/2} \left(\frac{\mu}{T} \right) + 2 \sum_{\nu=1}^\infty I_{-1/2} \left(\frac{\mu - \nu B}{T} \right) \right] \end{aligned} \quad (16)$$

(see figure 1) where the Fermi-Dirac integral for $k > -1$ is

$$I_k(x) = \int_0^\infty \frac{y^k}{e^{y-x} + 1} dy.$$

Using the relation $\frac{d}{dx} I_k(x) = k I_{k-1}(x)$ we obtain the pressure

$$P_{\text{el}}(\mu; T, B) = \frac{BT^{3/2}}{2^{1/2}\pi^2} \left[I_{1/2} \left(\frac{\mu}{T} \right) + 2 \sum_{\nu=1}^\infty I_{1/2} \left(\frac{\mu - \nu B}{T} \right) \right]. \quad (17)$$

It is evident that P_{el} and P'_{el} depend in a nontrivial way only on the ratios

$$\eta := \frac{\mu}{T} \quad \text{and} \quad \xi := \frac{B}{T}. \quad (18)$$

Moreover, if $\xi \ll 1$ (weak fields and/or high T) and η arbitrary, or $\xi \ll |\eta|$ (high or low densities) one may use the approximation

$$\xi \sum_{\nu=1}^\infty I_k(\eta - \nu\xi) \approx \int_0^\infty I_k(\eta - \xi)d\xi = \frac{1}{k+1} I_{k+1}(\eta). \quad (19)$$

Hence, in these limiting cases

$$P'_{\text{el}}(\mu; T) \approx \frac{2^{1/2}T^{3/2}}{\pi^2} I_{1/2} \left(\frac{\mu}{T} \right) \quad (20)$$

and

$$P_{\text{el}}(\mu; T) \approx \frac{2^{3/2} T^{5/2}}{3\pi^2} I_{3/2} \left(\frac{\mu}{T} \right), \quad (21)$$

are independent of B . At low densities, $\eta \rightarrow -\infty$, one may use the further approximation $I_{k+1}(\eta) \approx (k+1)!e^\eta$, and (20) and (21) reduce to the equation for a classical, ideal gas,

$$P_{\text{el}} = nT. \quad (22)$$

2.4. TF Theory in the Spherical Approximation

In the spherical approximation to TF theory of bulk matter each Wigner-Seitz cell is approximated by a sphere with the nucleus at the center. Thus, one considers (5), (6) and (7) with Ω a sphere of radius r_0 and a single nucleus with charge Z at $\mathbf{R}_1 = 0$. We consider only the neutral case, $N = Z$. Due to the spherical symmetry we may assume that Ψ depends only on the radial coordinate $r = |\mathbf{r}|$. To eliminate the nuclear charge Z we define

$$x = Z^{1/3} r, \quad (23)$$

$$\beta = \frac{B}{Z^{4/3}}, \quad \tau = \frac{T}{Z^{4/3}}, \quad (24)$$

and it is convenient to replace Ψ by

$$\Theta(x) = \frac{r\Psi(r)}{Z} = \frac{x\Psi(Z^{-1/3}x)}{Z^{4/3}}. \quad (25)$$

(Note that the dimensionless radial coordinate x is not the same as the one used in Paper I whereas the dimensionless potential Θ is the same.)

The TF equation (5) written in terms of these variables becomes

$$\frac{d^2\Theta(x)}{dx^2} = \frac{2^{1/2}}{\pi} \beta \tau^{1/2} x \left[I_{-1/2} \left(\frac{\Theta(x)}{x\tau} \right) + 2 \sum_{\nu=1}^{\infty} I_{-1/2} \left(\frac{\Theta(x)}{x\tau} - \frac{\nu\beta}{\tau} \right) \right]. \quad (26)$$

It has two parameters, β and τ .

The approximation (20) corresponds to

$$\frac{d^2\Theta(x)}{dx^2} = \frac{2^{5/2}}{\pi} \tau^{3/2} x I_{1/2} \left(\frac{\Theta(x)}{x\tau} \right). \quad (27)$$

It can be applied when either $\beta \ll \tau$ (high temperature and/or weak fields), or $\beta \ll \Theta/x$ (high density close to the nucleus).

The boundary condition (6) means that

$$\Theta(0) = 1 \quad (28)$$

and the boundary condition (8) is

$$\Theta'(x_0) = \frac{\Theta(x_0)}{x_0} \quad (29)$$

where $x_0 = Z^{1/3}r_0$, and the dash denotes differentiation with respect to x .

The pressure P_{TF} of bulk matter in the spherical TF approximation can be shown to be equal to the local electronic pressure at the boundary (Fushiki et al. 1989):

$$P_{\text{TF}} = P_{\text{loc}}(r_0) = P_{\text{el}}\left(\frac{Z^{4/3}\Theta(x_0)}{x_0}\right) \quad (30)$$

and the matter density ρ is simply given by:

$$\rho = \frac{Am_n}{(4\pi/3)r_0^3} = \frac{AZm_n}{(4\pi/3)x_0^3} \quad (31)$$

where A is the mass number and m_n is the nucleon mass. Combining (30) and (31) gives rise to the TF equation of state,

$$P_{\text{TF}} = P_{\text{TF}}(\rho; T, B). \quad (32)$$

In practice, one solves (26) with the initial condition (28) and a range of values for $\Theta'(0)$. In each case one then determines x_0 from (29). By varying $\Theta'(0)$ one obtains the necessary variation in the values of x_0 and hence of ρ (see e.g. figure 2).

The density and pressure profiles in an isothermal surface layer of a neutron star can be computed from the equation of state. The surface layer, where TF theory can reasonably be assumed to apply in a typical neutron star, is so thin that the gravitational acceleration g_s can be taken as constant. Denoting by z the depth from the surface, the equation of hydrostatic equilibrium for the pressure P is

$$\frac{dP}{dz} = \frac{dP}{d\rho} \frac{d\rho(z)}{dz} = g_s \rho(z). \quad (33)$$

Inserting (32) for P one may obtain $\rho(z)$ by integration (see a more detailed discussion of isothermal atmospheres in §4). As in Fushiki et al. (1989) and Paper I we find it more convenient, however, to express the equilibrium condition in terms of the atomic chemical potential,

$$\mu_{\text{atom}} = F_{\text{TF}} + P_{\text{TF}}v \quad (34)$$

where

$$F_{\text{TF}} = \int_{r \leq r_0} f_{\text{el}}(n_{\text{TF}}(\mathbf{r})) d^3\mathbf{r} - \int_{r \leq r_0} \frac{n_{\text{TF}}(\mathbf{r})}{r} d^3\mathbf{r} + \int_{r' \leq r_0} \int_{r \leq r_0} \frac{n_{\text{TF}}(\mathbf{r})n_{\text{TF}}(\mathbf{r}')}{|\mathbf{r} - \mathbf{r}'|} d^3\mathbf{r} d^3\mathbf{r}' \quad (35)$$

is the free energy per atom, and

$$v = (4\pi/3)r_0^3 \quad (36)$$

is the volume per atom. The equilibrium condition is (Fushiki et al. 1989)

$$\mu_{\text{atom}}(z) = \mu_{\text{atom}}(0) + Am_{\text{n}}g_{\text{s}}z. \quad (37)$$

If μ_{atom} is known as a function of the density ρ , this immediately gives $\rho(z)$ and hence also $P(z)$ from the equation of state.

In our calculations we have chosen to define the surface of the star to be where the matter density, ρ , matches the lowest density, ρ_0 , achieved in the zero temperature case. For each case of T and B used, we find the value of $\mu_{\text{atom}}(z=0) = \mu_{\text{atom}}(\rho = \rho_0)$. It is then easy to calculate the depth z for each value of ρ from equation (37) and hence evaluate $\rho(z)$ and $P(z)$. The results for isothermal atmospheres are shown in figures 9 and 10 and discussed further in §4. It should be kept in mind that free atoms cannot exist at $P = 0$ if $T > 0$, so there is no sharp surface.

2.5. Scaling Relations

The equations (26) and (29) have three parameters, $\beta = B/Z^{4/3}$, $\tau = T/Z^{4/3}$ and $x_0 = Z^{1/3}r_0$. By scaling they are equivalent to the original equations (5) and (8) with four parameters, Z , B , T and r_0 . From (17), (11), (34) and (35) we obtain the corresponding scaling relations for the pressure, the free energy and the atomic chemical potential. The matter density ρ (cf. equation (31)), is a more convenient variable than r_0 and we write the scaling relations in the following way:

$$P_{\text{TF}}(\rho, B, T; Z', A') = (Z'/Z)^{10/3} P_{\text{TF}}((ZA/Z'A')\rho, (Z'/Z)^{4/3}B, (Z'/Z)^{4/3}T; Z, A) \quad (38)$$

$$F_{\text{TF}}(\rho, B, T; Z', A') = (Z'/Z)^{10/3} F_{\text{TF}}((ZA/Z'A')\rho, (Z'/Z)^{4/3}B, (Z'/Z)^{4/3}T; Z, A) \quad (39)$$

$$\mu_{\text{atom}}(\rho, B, T; Z', A') = (Z'/Z)^{7/3} \mu_{\text{atom}}((ZA/Z'A')\rho, (Z'/Z)^{4/3}B, (Z'/Z)^{4/3}T; Z, A) \quad (40)$$

These relations allow us to compute the pressure, free energy and chemical potential for any pair (Z', A') if it is known for some reference pair (Z, A) as e.g. for iron with $Z = 26$, $A = 56$.

2.6. Limiting cases and validity

There are three limiting cases, where TF theory simplifies and eventually passes over into the theory of a noninteracting electron gas. In terms of the parameters $\beta = B/Z^{4/3}$, $\tau = T/Z^{4/3}$ and $x_0 = Z^{1/3}r_0$ these cases are:

- High density limit: $x_0(1 + \beta)^{2/5} \ll 1$.
- High temperature limit: $\tau/(1 + \beta)^{2/5} \gg 1$.
- Low density limit: $\tau \ln x_0/(1 + \beta)^{2/5} \gg 1$.

To understand these limits one should recall that for an isolated TF atom at $T = 0$ the radius $r_{B,Z}$ is of the order $Z^{-1/3}(1 + \beta)^{-2/5}$ and the ground state energy $E(B, Z)$ of the order $-Z^{7/3}(1 + \beta)^{2/5}$ (Fushiki et al. 1992). The high density limit corresponds therefore to $r_0 \ll r_{B,Z}$, i.e. highly compressed matter. The high temperature limit means that $T \gg |E(B, Z)|/Z$, i.e. the thermal energy is much larger than the ground state energy per electron for isolated atoms. The low density limit is mainly of interest as a check for the correctness of the numerical computations. In this limit the electron gas is essentially a classical ideal gas of density $n \sim r_0^{-1/3}$, because the chemical potential $\sim T \ln n$ of free electrons is much lower than the chemical potential $\sim E(B, Z)/Z$ of electrons bound to the nuclei.

In the three limiting cases TF theory may be compared with the simpler *uniform model* (see, e.g., Fushiki et al. 1989 and Paper I), defined by the free energy

$$F_u(\rho; B, T) = \frac{M}{\rho} f_{\text{el}}((Z/M)\rho; B, T) - \frac{9}{10} Z^2 \left(\frac{\rho}{M} \right)^{1/3}, \quad (41)$$

where $M = Am_n$ and we use ρ as a variable instead of r_0 . The mean electron density is $(Z/M)\rho$, and the first term in (41) is the free energy of a ball of radius r_0 of a uniform, noninteracting electron gas, whereas the second term is the Coulomb energy of the ball, due to electronic repulsion and attraction of the nucleus. The pressure in the uniform model is

$$P_u(\rho; B, T) = P_{\text{el}}((Z/M)\rho; B, T) - \frac{3}{10} \left(\frac{4\pi}{3} \right)^{1/3} Z^2 \left(\frac{\rho}{M} \right)^{4/3}, \quad (42)$$

with P_{el} given by (17). Since P_{el} behaves like $\rho^{5/3}$ at high ρ and as ρT at small ρ or high T it is also clear that the first term in (42) dominates over the second in the limiting cases considered. A comparison of P_{TF} with P_u and P_{el} is shown in figure 6.

In Hauksson (1996) the status of TF theory with a magnetic field at nonzero temperature as an approximation of quantum mechanics is investigated, generalizing the zero temperature limit theorems of Lieb et al. (1994). It is found that thermodynamical functions calculated from quantum mechanics converge to the corresponding functions in TF theory in the limit when the nuclear charge Z and the magnetic field B tend to infinity, provided $B/Z^3 \ll 1$. The temperature T and the radius r_0 are in this limit scaled in such a way that $\tau/(1 + \beta)^{2/5}$ and $x_0(1 + \beta)^{2/5}$ are fixed, i.e. T scales as $Z^{4/3}(1 + (B/Z^{4/3}))^{2/5}$ and r_0 as $Z^{-1/3}(1 + (B/Z^{4/3}))^{-2/5}$. In compressed matter and/or at high temperature the condition $B/Z^3 \ll 1$ can be relaxed. In fact by the heuristic argument in Paper I, TF theory for compressed matter at zero temperature, i.e. for $r_0 < Z^{-1/3}(1 + (B/Z^{4/3}))^{-2/5}$, can be expected to be a good approximation, if $Z \gg 1$ and $B \ll Z/r_0^2$. If $T \gg B$, many Landau levels are excited, and the magnetic field becomes irrelevant. Hence at such extreme temperatures the condition for validity is simply $Z \gg 1$. Summing up, the domain of validity of TF theory at non-zero temperature should be at least as large as that for zero temperature illustrated in Fig. 1 in Paper I, and strictly larger for $T > B$.

3. Numerical Methods

Since the calculations presented in this article are an extension of those presented in Paper I, the numerical methods are in most aspects similar. The details given in that paper will not be repeated, but here we present a general outline together with considerations specific to the case of non-zero temperatures.

To solve the TF equation (5) numerically, we use a fourth-order Runge-Kutta method with adaptive stepsize control (Press et al. 1992) with the boundary conditions (28) and (29). First we pick a suitable spectrum of values of $\Theta'(0)$ and then integrate outwards from $\Theta(0)$ until condition (29) is satisfied. We then know both x_0 and $\Theta(x_0)$ which we can use to calculate the density and the chemical potential, and hence the corresponding pressure for a given temperature and magnetic field.

It is worth mentioning some changes from the zero temperature case. The kinetic energy density, denoted by w in Paper I, is replaced with the free energy density, f . Whereas w is always non-negative, the free energy density can become negative because of the added temperature term. This allows the electrochemical potential Θ to become negative for high temperatures and low densities, since in such cases the free energy, f , can have a negative derivative with respect to n , yielding $\mu < 0$. An example of this is seen in figure 2 where we plot Θ as a function of x for two different densities and temperatures with B fixed. Also, when $T > 0$ there are no free atoms at $P = 0$, contrary to the case for zero temperature (e.g. Paper I).

As in Paper I, we chose to include the first 100 terms of the infinite sums in the formulas (16) and (17) for n and P ensuring a relatively high precision without too much computational cost. Here, we encountered a similar divergence problem as in the zero temperature case; close to the nucleus, both n and μ tend to infinity. We also found the convergence of the sums in (16) and (17) to be slow for magnetic fields low compared to the temperature. Both problems may be solved by using the approximations (20) and (21), since in the first case $\xi \ll |\eta|$ and in the second $\xi \ll 1$. It then remains to find a criteria for where to switch over to these approximations. It is convenient to rewrite the expressions depending on μ in equations (16) and (17) as

$$\left[I_k(\xi\zeta) + 2 \sum_{\nu=1}^{\infty} I_k(\xi(\zeta - \nu)) \right]$$

with

$$\zeta := \frac{\mu}{B}$$

and determine in terms of ζ and ξ where to switch over to the approximations to obtain the desired accuracy. We decided that in the worst case the relative error in P and n should never exceed 2×10^{-4} for any value of μ at a given temperature and magnetic field strength. We calculated this error for the two methods, using only 100 Landau levels on one hand and the approximations on the other and comparing the results with the values obtained with 5000 Landau levels (which we consider as exact). This comparison yielded critical values for ζ , referred to as ζ_c , above which

the approximations (20) and (21) are used instead of the partial sum over 100 levels (see table 1). Since different Fermi-Dirac integrals enter the calculations of n and P , slightly different ζ_c values are appropriate in each case for the same ξ . The Fermi-Dirac integrals were evaluated using the method of Cody & Thatcher (1967) which assures a relative error less than 3×10^{-9} . (Note that in their paper, the value of q_s for $s = 0$ and $n = 4$ in table IIC should read 1.00 and not 1.05.)

4. Results

In this section we present the results of our numerical TF calculations for bulk matter in high magnetic fields and at finite temperature. We remind the reader that our reference element is iron with $Z = 26$ and $A = 56$ and that the treatment is non-relativistic. Hence the highest density used in our calculations is 10^6 g cm^{-3} and the highest temperature is 100 keV ($1.16 \times 10^9 \text{ K}$). As in Paper I the range in magnetic field strength is from 10^{10} to 10^{13} G. The reason for this is that in the case of iron one obtains the zero-field results (see e.g. Abrahams & Shapiro 1991) if the fields are much weaker than 10^{10} G whereas for field strengths slightly higher than 10^{12} G essentially only the lowest Landau level is populated and one obtains the results of Constantinescu & Moruzzi (1978) and Abrahams & Shapiro (1991).

Our presentation of results is mainly in graphical form but tabulated results are available at the website <http://www.raunvis.hi.is/~ath/TFBT>. By use of the scaling relations discussed in §2.5 the numerical TF results can also be used for elements other than iron and for different temperatures and magnetic field strengths.

Figure 3 shows a typical example of how temperature changes the electron distribution inside a unit iron cell of a given size, corresponding to fixed matter density. The quantity plotted is $r^2n(r)$ which is useful since the the number of electrons in a shell is proportional to the area under the corresponding curve. The case shown is for a field strength of 10^{11} G and a density of 1000 g cm^{-3} . The main thing to notice is that thermal effects tend to smooth out the distinct Landau shell structure which is so prominent in the zero temperature case (see Fushiki et al. 1992, and Paper I). However, as long as the temperature is lower than approximately one tenth of the cyclotron energy, $\hbar\omega_B$ ($\approx 11.58B_{12} \text{ keV}$ where $B_{12} = B/10^{12} \text{ G}$), thermal effects are not particularly pronounced. It is only when the temperature is comparable to or higher than the cyclotron energy ($\approx 1 \text{ keV}$ for 10^{11} G) that the electron distribution becomes drastically different from the zero temperature case. This is a reflection of the temperature dependence of the relation between n and μ for the free electron gas shown in figure 1. From figure 3 it is also clear that the number density of electrons at the edge of the unit cell increases with increasing temperature and thus the TF pressure of bulk matter at given matter density and field strength also increases with temperature.

In figures 4 to 10 we present the results of our calculations of the bulk properties of dense matter. Figure 4 shows the TF equation of state for iron, P_{TF} versus ρ , where P_{TF} is given by

equation (30) and ρ by equation (31). Each curve corresponds to a fixed value of the temperature. The presence of a Landau shell structure in the electron distribution is reflected in a clear oscillatory nature of the pressure-density relationship as long as the temperature is lower than approximately one tenth of the cyclotron energy (i.e. $T \leq 1B_{12}\text{keV}$). For somewhat higher temperatures the oscillations are smoothed out as previously noted by Gadiyak et al. (1981).

In figure 4c we compare the TF equation of state for a field strength of 10^{12} G with that of a nondegenerate gas of free electrons with uniform density $n = Z\rho/Am_n$ and temperature T but in zero magnetic field. This pressure is given by equation (22) or equivalently by

$$P_{\text{class}} = P_{\text{class}}(\rho, T, B = 0) = Z\rho kT/Am_n, \quad (43)$$

where we use the notation P_{class} instead of P_{el} in order to avoid confusion with the more general expressions for P_{el} in §2.3 (also note the change of units from those used in §2). We have chosen the value of 10^{12} G for this particular discussion but the same qualitative features are present for all B . Figure 4c shows that at low densities the magnetic TF pressure approaches P_{class} for fixed B and T . The same is true in the limit of high temperatures at fixed ρ and B . Hence at very low densities and/or very high temperatures the TF pressure becomes independent of B as expected from the discussion of asymptotic behaviour in §2.6. On the other hand at high enough densities and as long as the temperature does not become too high both thermal and magnetic effects on the equation of state become negligible and it approaches the non-magnetic TF equation of state of iron at zero temperature (Paper I). This limiting behaviour is clearly seen in figure 5 which shows P_{TF} versus ρ for $T = 0.1$ keV and several values of the magnetic field.

In figure 6 we compare the TF pressure, P_{TF} , with P_u , the pressure of the uniform model discussed in §2.6 (see equation (42)). Results are shown for a magnetic field with strength 10^{12} G and two values of the temperature. Also shown is the pressure of a noninteracting electron gas, P_{el} , given by equation (17). It is clear from the figures that the three models have the same behaviour in the limit of high or low densities and at high temperatures as already discussed in §2.6. The differences between the different approximations are greatest at low temperatures and in a restricted range of relatively low densities. This is approximately the range in which one expects contributions from the thermal motion of the nuclei to be important (see the discussion below).

For completeness we show in figure 7 the Thomas-Fermi free energy for iron in bulk, F_{TF} , as a function of ρ for selected values of T and B (see equation (35)).

At this point we would like to mention a few corrections to the equation of state that go beyond the TF approximation and are therefore not included in our calculations. For further discussion of this and related topics we refer the reader to Paper I and the papers by Fushiki et al. (1992) and Yakovlev & Kaminker (1994).

As already mentioned in the introduction the pure TF method neglects both exchange effects between the electrons as well as “gradient corrections” of the von Weizsäcker type. Although these effects are not expected to make much difference as far as bulk properties of matter are

concerned (Fushiki et al. 1992) it should be kept in mind that they may become important at very low temperatures and the densities corresponding to the surface densities of neutron stars (Fushiki et al. 1989; Abrahams & Shapiro 1991; Paper I). To investigate this in detail requires more exact calculations than are provided by the one dimensional (spherical) TF method.

An additional simplification is that in TF theory the nuclei are assumed to be stationary at fixed relative distances determined by the matter density, their number density given by $n_i = \rho/Am_n$. Thus the thermal motion of the nuclei is neglected in calculations of the TF pressure. This motion is only weakly affected by the magnetic field and for most applications of relevance to the investigation of neutron star envelopes it is a fairly good approximation to regard the nuclei as forming an ideal non-degenerate gas with pressure

$$P_i = n_i kT = \rho kT / Am_n \quad (44)$$

(for a more detailed discussion see e.g. Gudmundsson et al. 1983, and Yakovlev & Kaminker 1994). Note however that $P_i = P_{\text{class}}/Z$, where P_{class} is the pressure of the ideal non-degenerate gas of electrons at the same ρ and T (see equation (43)) and thus the pressure of the nuclei is small compared to the TF pressure except at low temperatures and low densities, which are of little importance for compressed matter. This can e.g. be seen by inspecting figures 4c and 6 which show a comparison between P_{TF} , P_{class} , P_{el} , and P_{u} for $B = 10^{12}$ G. We thus feel justified in neglecting the thermal motion of the nuclei in our calculations. We point out however that in case one wants to include the contribution of the nuclei to the total pressure and chemical potential this can easily be done by adding them to the TF results, thus obtaining

$$P = P_{\text{TF}} + P_i \quad (45)$$

and

$$\mu = \mu_{\text{atom}} + \mu_i, \quad (46)$$

where μ_{atom} is given by equation (34). For an ideal non-degenerate gas of nuclei in zero magnetic field P_i is given by equation (44) above and

$$\mu_i = kT \ln [n_i (2\pi\hbar^2/m_n kT)^{3/2}]. \quad (47)$$

A more detailed treatment taking into account the non-ideal behaviour of nuclei due to Coulomb interactions between nuclei and quantum effects is beyond the scope of this paper. We would however like to remind the reader that these effects are expected to make only relatively small corrections to the equation of state of bulk matter for most of the temperatures and densities of interest in the study of neutron star envelopes. On the other hand they do have a considerable influence on the transport properties in magnetic neutron stars, and they also determine which form or phases of matter are present in the envelope (see e.g. Gudmundsson et al. 1983; Van Riper 1988; Yakovlev & Kaminker 1994; Lai & Salpeter 1997, and references therein).

We now return to the discussion of the results of our TF calculations. Figure 8 shows the isothermal sound velocity,

$$a_T = \left(\frac{\partial P}{\partial \rho} \right)_T^{1/2} \quad (48)$$

with $P = P_{\text{TF}}$, as a function of density for several values of the temperature and a magnetic field of 10^{12} G. This quantity is related to the adiabatic sound velocity $a_s = (\partial P / \partial \rho)_s^{1/2}$ by

$$a_T^2 = \frac{c_v}{c_p} a_s^2,$$

where c_p and c_v are the specific heats at constant pressure and volume, respectively. As discussed in Paper I (see also Landau & Lifshitz 1960) a_s is the velocity of longitudinal magnetosonic waves when the wavevector is parallel to the magnetic field. Figure 8 shows that the oscillatory behaviour which is due to the Landau shell structure in the electronic density distribution of the unit cells is clearly present in a_T at finite temperatures. Even though thermal effects tend to smooth them out they are quite pronounced as long as the temperature is less than approximately one tenth of the cyclotron energy. It is only when the temperature is of order $10 B_{12}$ keV or higher that the oscillations disappear completely, an effect that has already been discussed in connection with the equation of state. In two or three dimensional TF calculations an additional smoothing effect would probably be present due to the non-spherical nature of the unit cells. However as argued in Paper I they would not be big enough to wipe out the oscillations.

These de Haas-van Alphen type oscillations are reflected in the isothermal compressibility of bulk matter κ_{bulk} , which is related to the sound velocity by

$$\kappa_{\text{bulk}} = \frac{1}{\rho a_T^2}, \quad (49)$$

and hence they are also present in the density and pressure profiles of matter in the surface layers of neutron stars (Paper I). In most cases of interest the temperature in the surface layers rises quite steeply as a function of depth and hence the oscillatory behaviour in the matter density can not be investigated in detail without solving the thermal structure equations of the envelope. This requires knowledge of the opacity as well as the equation of state (Gudmundsson et al. 1983; Van Riper 1988). Some insight may clearly be gained however by considering the simplified case of isothermal surface layers, an approximation which may in fact be appropriate for sufficiently old and relatively cold neutron stars. Figures 9 and 10 show the results of such isothermal structure calculations for a range of temperatures and two values of the magnetic field strength. The method used in the calculations is that described at the end of §2.4. The oscillatory behaviour is clearly seen in figure 9 as steps in the density profiles for the lowest temperatures whereas the effect is somewhat weaker in the pressure profiles in figure 10. Notice also that at high temperature both the density and pressure gradients are very small in the outermost layers. This is a result of the fact that there is no sharp boundary at $T > 0$. For this reason the depth shown in figures 9 and 10 is measured from the point where the surface would be at zero temperature (see the discussion at the end of §2.4 and Paper I).

In some applications it is also of interest to know the column density, σ , either as a function of zg_s or of ρ . In either case it is easy to calculate the column density from the surface to the point in the star where the pressure is P since it is simply given by the expression

$$\sigma - \sigma_s = \int_0^z \rho dz' = \int_{P_s}^P \frac{dP'}{g_s} = (P - P_s)/g_s, \quad (50)$$

where we have used equation (33) and σ_s and P_s are the column density and pressure at the surface of the neutron star, respectively. Hence the results shown in figures 4 and 10 can easily be used for evaluating σ .

We end the discussion of our results by estimating the effects of the thermal motion of the nuclei on the velocity of sound and hence also on κ_{bulk} and the isothermal surface structure. If we assume as before that the nuclei form an ideal non-degenerate gas at temperature T then by use of equations (44) and (48) we find that the TF sound velocity shown in figure 8 and denoted by a_T has to be replaced by a'_T given by

$$a'_T = (a_T^2 + kT/Am_n)^{1/2}. \quad (51)$$

By comparing the nuclear contribution, $(kT/Am_n)^{1/2} \approx 4 \times 10^6 (T/\text{keV})^{1/2}$ cm/s, to the values of a_T shown in figure 8 one can see as before that it is only at the lowest temperatures and in a restricted range of low densities that the thermal motion of the nuclei needs to be taken into account. In particular it is clear that this motion has a negligible effect on the high density oscillatory behaviour which occurs at low temperatures.

5. Conclusions

In this paper we have presented the results of a detailed calculation of the properties of hot dense matter in high magnetic fields using the temperature dependent Thomas-Fermi method and taking all Landau levels into account. By including temperature these calculations extend our previous work on the properties of cold dense matter in the TF approximation presented in Paper I.

On the grounds discussed in Fushiki et al. (1992) and Paper I we expect that TF theory catches the main features of bulk matter composed of heavy elements like iron. This applies also for finite temperatures and high magnetic fields up to at least a few times 10^{12} G.

We have investigated the range of validity of the finite temperature TF model for matter in a magnetic field and estimated the effects of the thermal motion of nuclei on the properties of matter in bulk. We find that the nuclear contribution to the total pressure and other bulk properties is very small except in a restricted range of low densities and low temperatures.

Within the range of validity of the finite temperature TF theory we have found that the Landau shell structure which is so pronounced in iron at zero temperature is also present at

finite temperature as long as it does not exceed about one tenth of the cyclotron energy. This structure is reflected in an oscillating component of the de Haas-van Alphen type in all the bulk properties of matter as functions of depth in isothermal surface layers of magnetic neutron stars. At temperatures around the cyclotron energy or higher, thermal effects smooth out the oscillations. Further investigation of this problem including the additional effects of smoothing of oscillations due to the non-spherical shape of the unit cells requires two or three dimensional TF calculations. Furthermore an investigation of the thermal structure of the surface layers when the assumption of isothermality is not valid requires solving the thermal structure equations of neutron star envelopes. This in turn requires knowledge of the transport properties of matter in high magnetic fields in addition to the equation of state presented in this work. Such study is beyond the scope of this paper. Finally we remind the reader that our numerical results are available in tabular form at the website <http://www.raunvis.hi.is/~ath/TFBT>.

We are grateful to Chris Pethick and Sasha Potekhin for valuable discussions. A. Th. and E. H. G. would like to thank Nordita for generous hospitality. J. Y. acknowledges a grant from the Adalsteinn Kristjánsson Foundation of the University of Iceland. This work was partially supported by the Research Fund of the University of Iceland and by Danmarks Grundforskningsfond through its support of the Theoretical Astrophysics Center.

References

- Abrahams, A. M., Shapiro, S. L. 1991, *ApJ*, 374, 652
- Chabrier, C., Potekhin, A. Y., Yakovlev, D. G. 1997, *ApJ*, 477, L99
- Cody, W. J., Thatcher, H. C. 1967, *Math. Comp.*, 21, 30
- Constantinescu, D. H., Moruzzi, G. 1978, *Phys. Rev. D*, 18, 1820
- Fushiki, I., Gudmundsson, E. H., Pethick, C. J. 1989, *ApJ*, 342, 958
- Fushiki, I., Gudmundsson, E. H., Pethick, C. J., Yngvason, J. 1992, *Ann. Phys.*, 216, 29
- Gadiyak, G. V., Obrecht, M. S., Yanenko, N. N. 1981, *Astrophysics*, 17, 416
- Gudmundsson, E. H., Pethick, C. J., Epstein, R. I. 1983, *ApJ*, 272, 286
- Hauksson, B. 1996, *Master's thesis*, University of Iceland
- Hernquist, L. 1985, *MNRAS*, 213, 313
- Lai, D., Salpeter, E. E. 1997, *astro-ph/9704130*
- Landau, L. D., Lifshitz, E. M. 1960, *Electrodynamics of Continuous Media*, Oxford: Pergamon
- Lieb, E. H., Solovej, J., Yngvason, J. 1994, *Commun. Math. Phys.*, 161, 77
- Nomoto, K., Tsuruta, S. 1987, *ApJ*, 312, 711
- Page, D. 1995, *ApJ*, 442, 273
- Pavlov, G., Shibano, Y. A., Zavlin, V. E., Mayer, R. 1995, in M. A. Alpar, Ü. Kiziloğlu, J. van Paradijs (eds.), *The Lives of the Neutron Stars*, Dordrecht: Kluwer, 101
- Pethick, C. J. 1992, *Rev. Mod. Phys.*, 64, 1133
- Potekhin, A., Chabrier, C., Yakovlev, D. G. 1997, *A&A*, in press
- Potekhin, A. Y. 1996, *A&A*, 306, 999
- Potekhin, A. Y., Yakovlev, D. G. 1996, *A&A*, 314, 341
- Prakash, M., Bombaci, I., Prakash, M., Ellis, P. J., Lattimer, J. M. 1997, *nucl-th/9603042*, to appear in *Phys. Rep.*
- Press, W. H., Teukolsky, S. A., Vetterling, W. T., Flannery, B. P. 1992, *Numerical Recipes*, Cambridge University Press, 2nd edition
- Rögnvaldsson, Ö. E., Fushiki, I., Gudmundsson, E. H., Pethick, C., Yngvason, J. 1993, *ApJ*, 416, 276
- Schaaf, M. E. 1990a, *A&A*, 227, 61

Schaaf, M. E. 1990b, *A&A*, 235, 499

Umeda, H., Tsuruta, S., Nomoto, K. 1994, *ApJ*, 433, 256

Van Riper, K. A. 1988, *ApJ*, 329, 339

Yakovlev, D. G., Kaminker, A. D. 1994, in G. Chabrier, E. Schatzman (eds.), *Equation of State in Astrophysics*, Cambridge: Cambridge Univ. Press, 214

B/T	0.0001	0.001	0.01	0.1	1	10	100
n	-	-	32	97	97	97	97
P	-	50	97	97	97	97	97

Table 1: Values of ζ_c . For $\zeta > \zeta_c$ approximations (20) and (21) are used when calculating n and P , respectively. Where no value is given, the approximations are used for all values of ζ . Here, B is measured in units of 10^{12} G and T in keV.

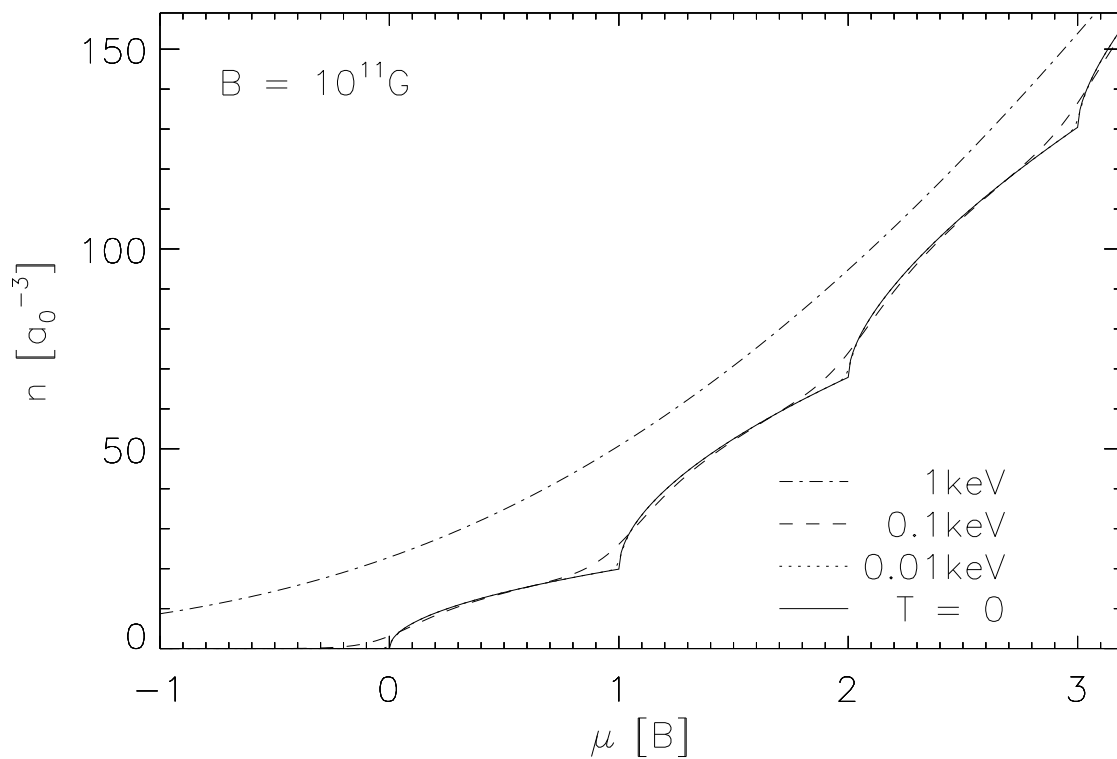


Fig. 1.— The electron number density as a function of the chemical potential for a uniform gas of free electrons. The curves are drawn for $B = 10^{11}$ G and three temperatures between 0.01 keV and 1 keV in addition to the zero temperature case. Note that the Landau band structure which is still present at $T = 0.01$ keV has almost disappeared at $T = 0.1$ keV and is not visible at $T = 1$ keV. The quantities on the axes are dimensionless: n is written in units of a_0^{-3} and μ in units of the cyclotron energy (equal to B in dimensionless units).

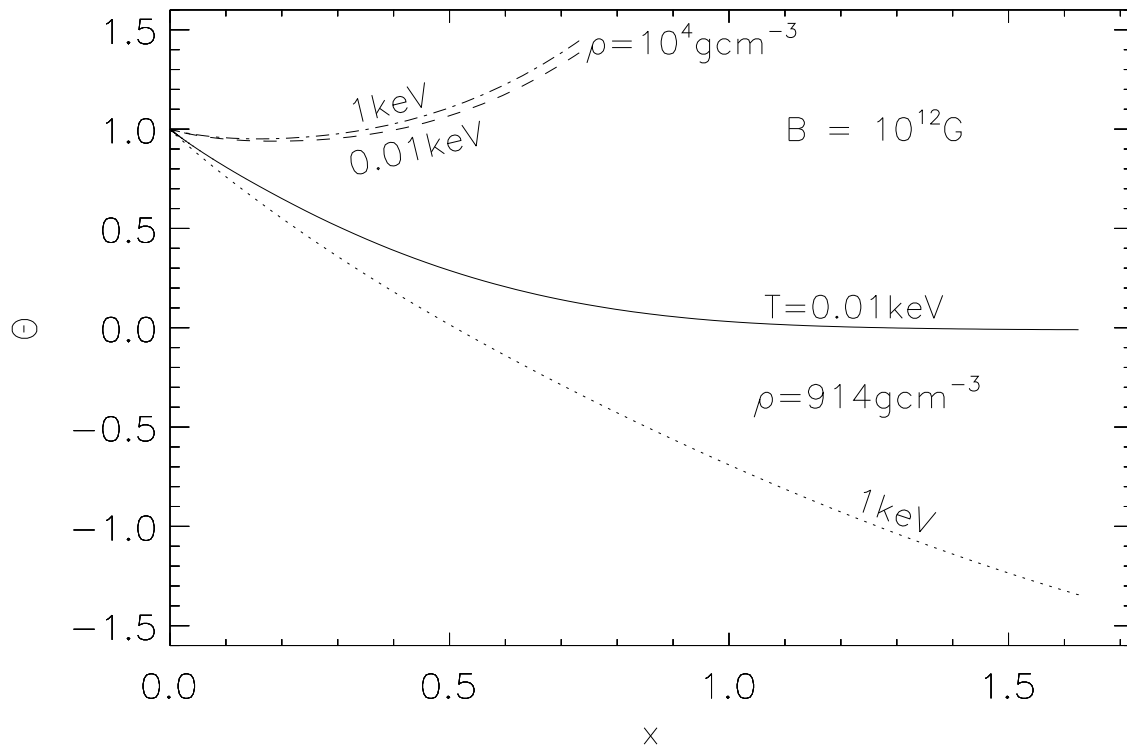


Fig. 2.— The potential Θ as a function of the radial coordinate x for two unit cells corresponding to two different values of the matter density. Results are shown for two values of temperature and a magnetic field strength of 10^{12} G. The behaviour of Θ for $T = 0.01$ keV is very similar to the zero temperature case. Note that for higher temperatures, such as $T = 1$ keV shown here, Θ becomes negative at the low matter density whereas at the higher density it takes values which are higher than in the zero temperature case.

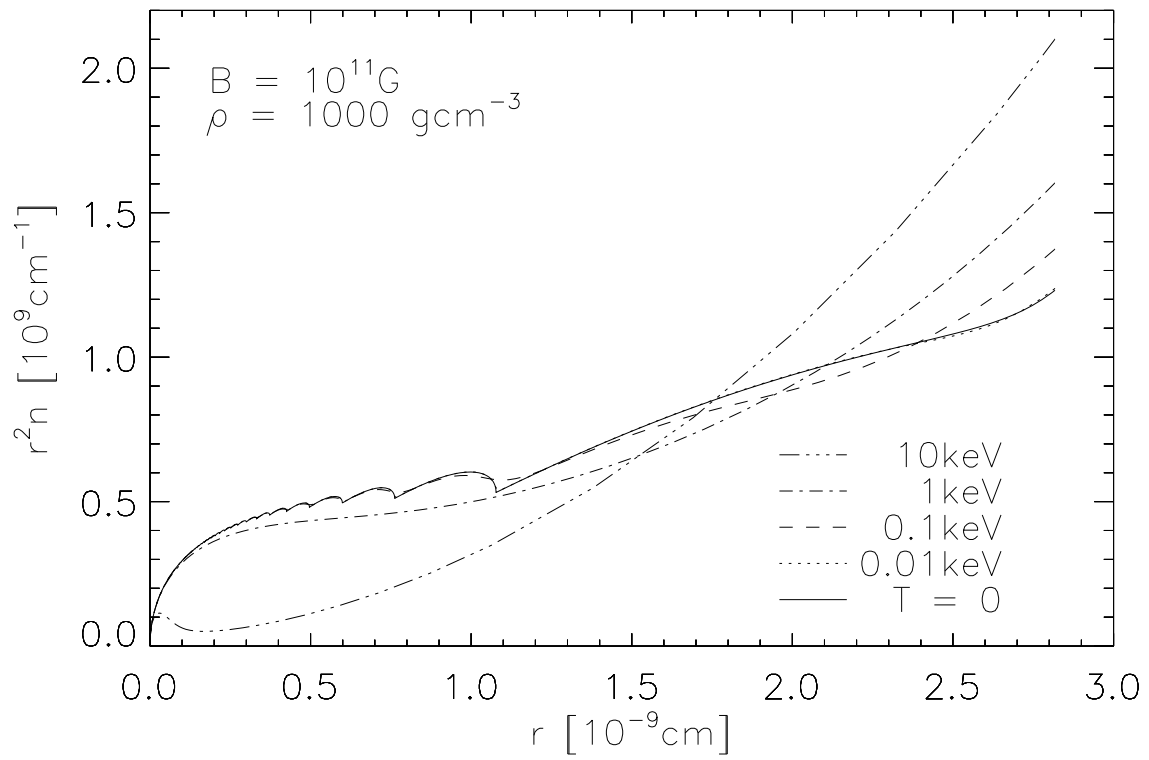


Fig. 3.— The quantity $r^2 n$ for a spherical unit cell of iron in the TF approximation. The matter density is 1000g cm^{-3} and the magnetic field strength 10^{11}G . Results are shown for five different values of the temperature.

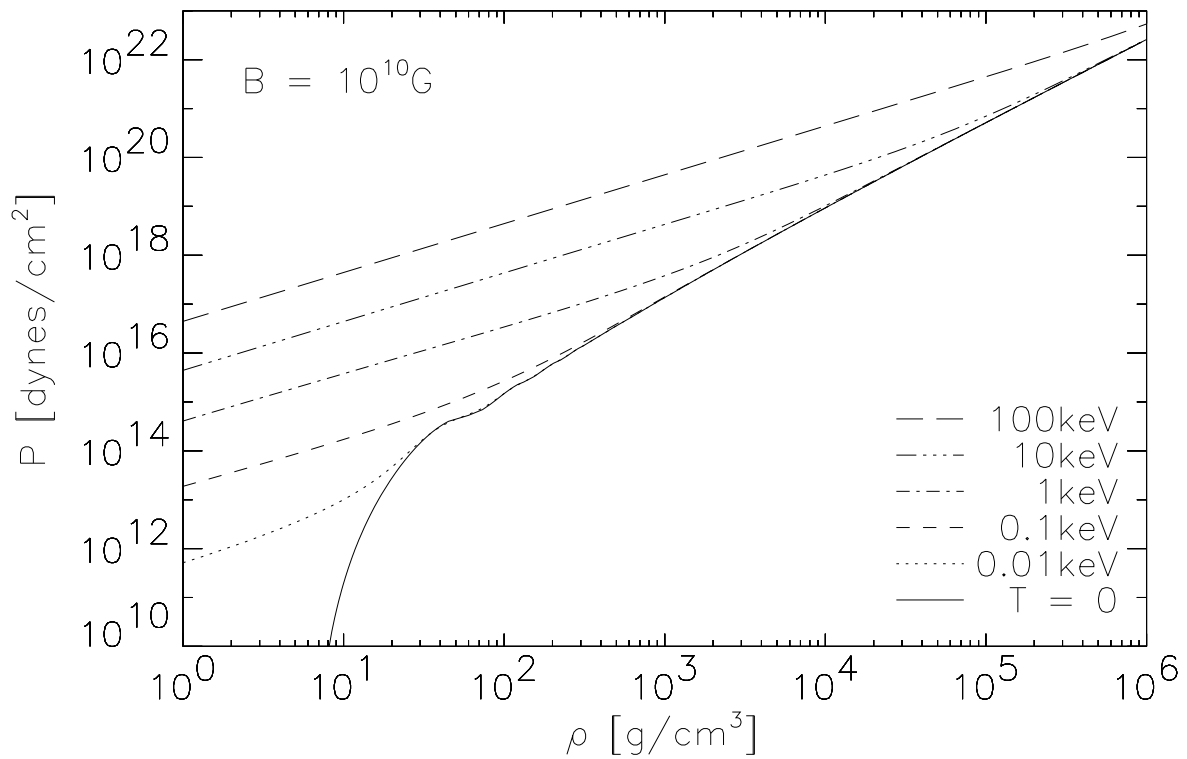


Fig. 4a.— The Thomas-Fermi equation of state for iron in a magnetic field. In each case results are shown for six values of the temperature, including the zero temperature case. (a) $B = 10^{10}$ G. (b) $B = 10^{11}$ G. (c) $B = 10^{12}$ G. (d) $B = 10^{13}$ G. In 4c the pressure of an ideal non-degenerate gas of free electrons in zero field, P_{class} , is superimposed on the TF results for comparison. See the text for further explanation.

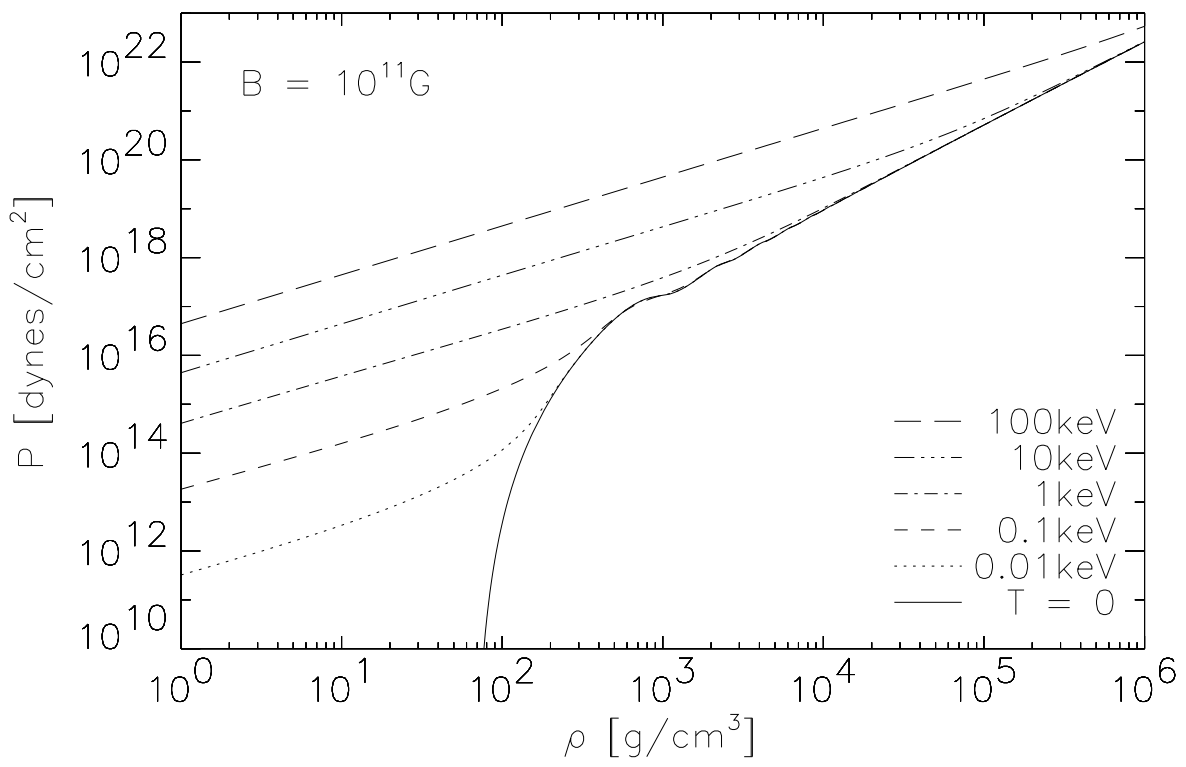


Fig. 4b.—

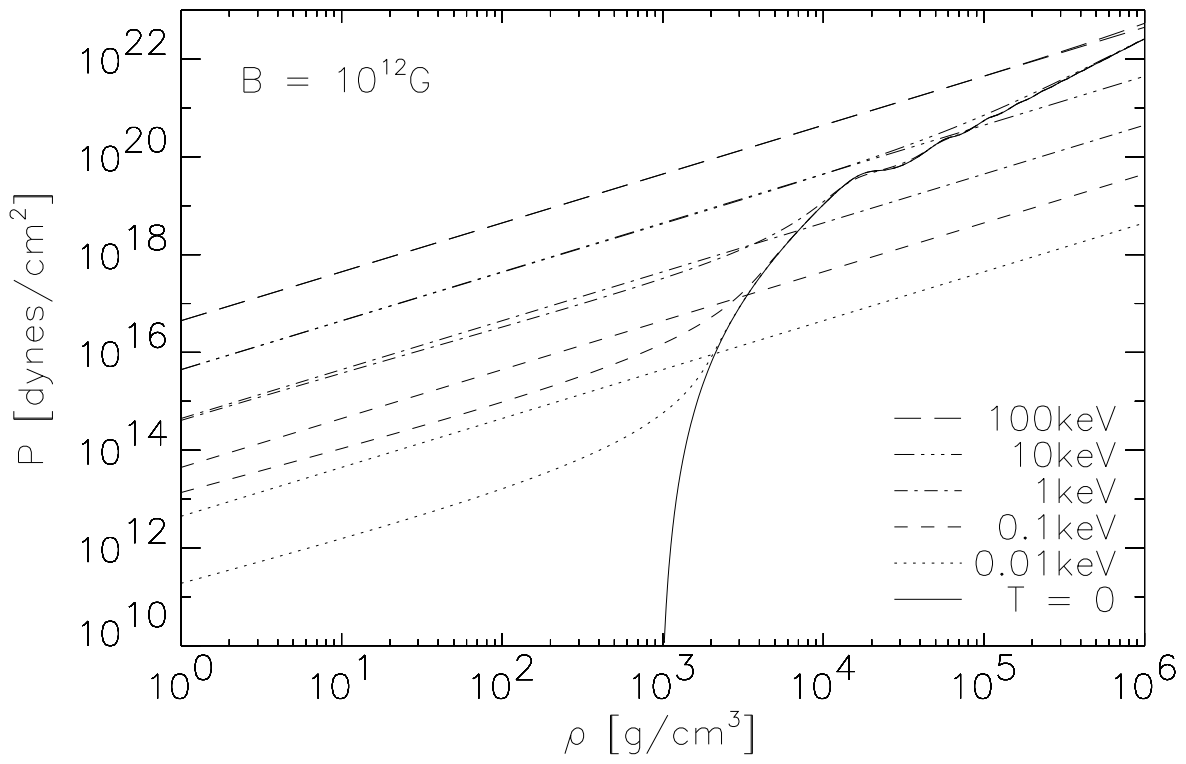


Fig. 4c.—

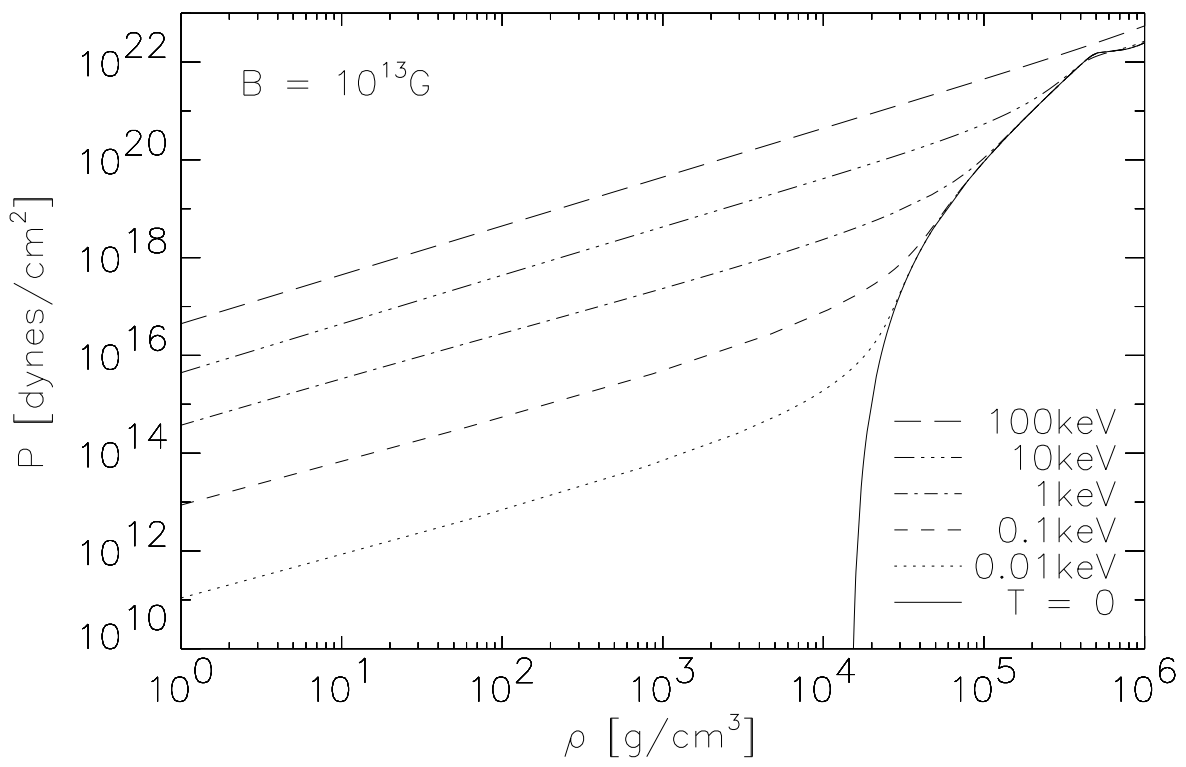


Fig. 4d.—

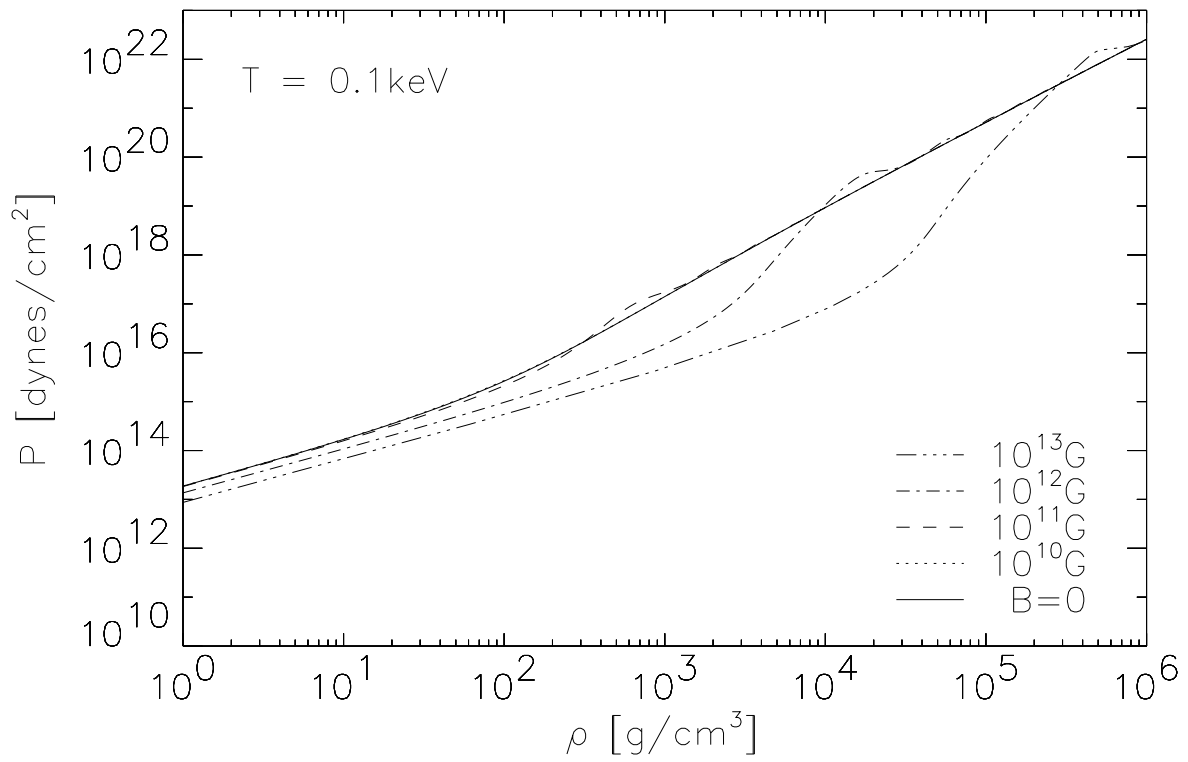


Fig. 5.— The Thomas-Fermi equation of state for iron at a temperature of 0.1 keV and several values of the magnetic field strength. Note in particular that the curve for $B = 10^{10}$ G falls almost completely on top of the zero field curve.

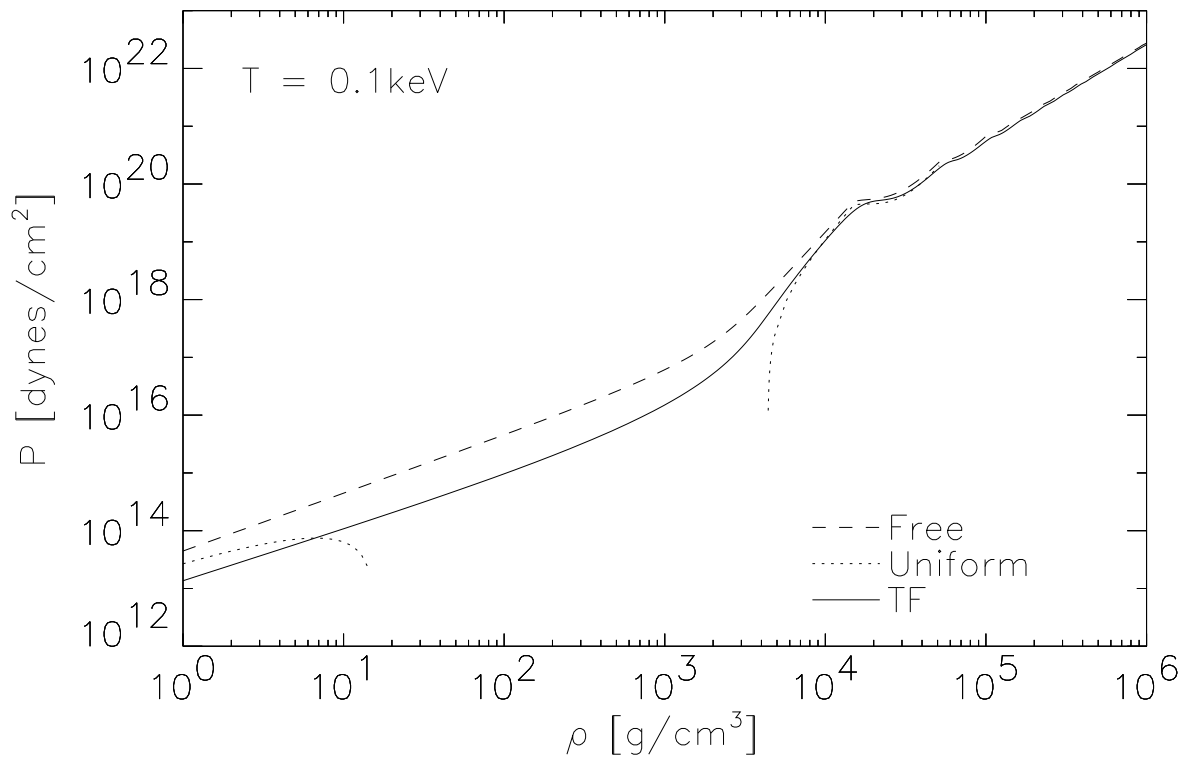


Fig. 6a.— The equation of state for iron in three different approximations. The TF pressure, P_{TF} , is shown by the solid line. The pressure of a Fermi gas of free electrons, P_{el} , is shown by the dashed line and the pressure in the uniform model, P_{u} , by the dotted line. The strength of the magnetic field is 10^{12} G. (a) $T = 0.1$ keV. (b) $T = 1$ keV.

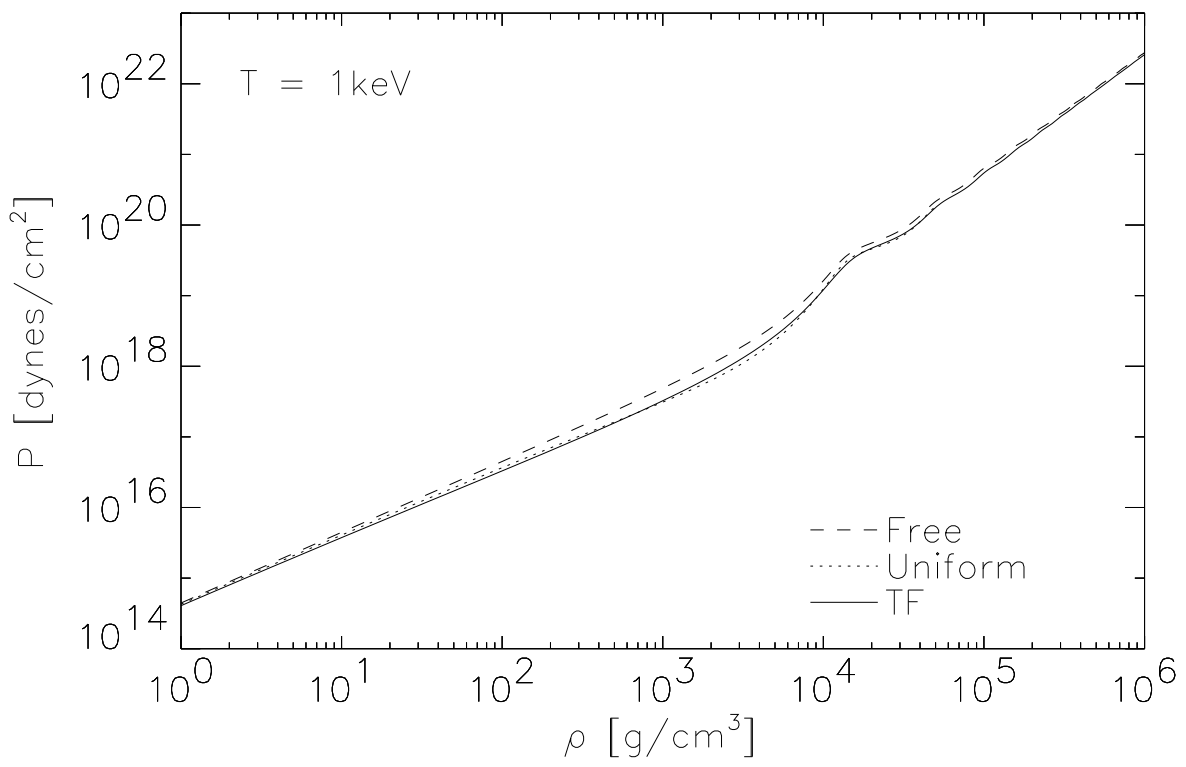


Fig. 6b.—

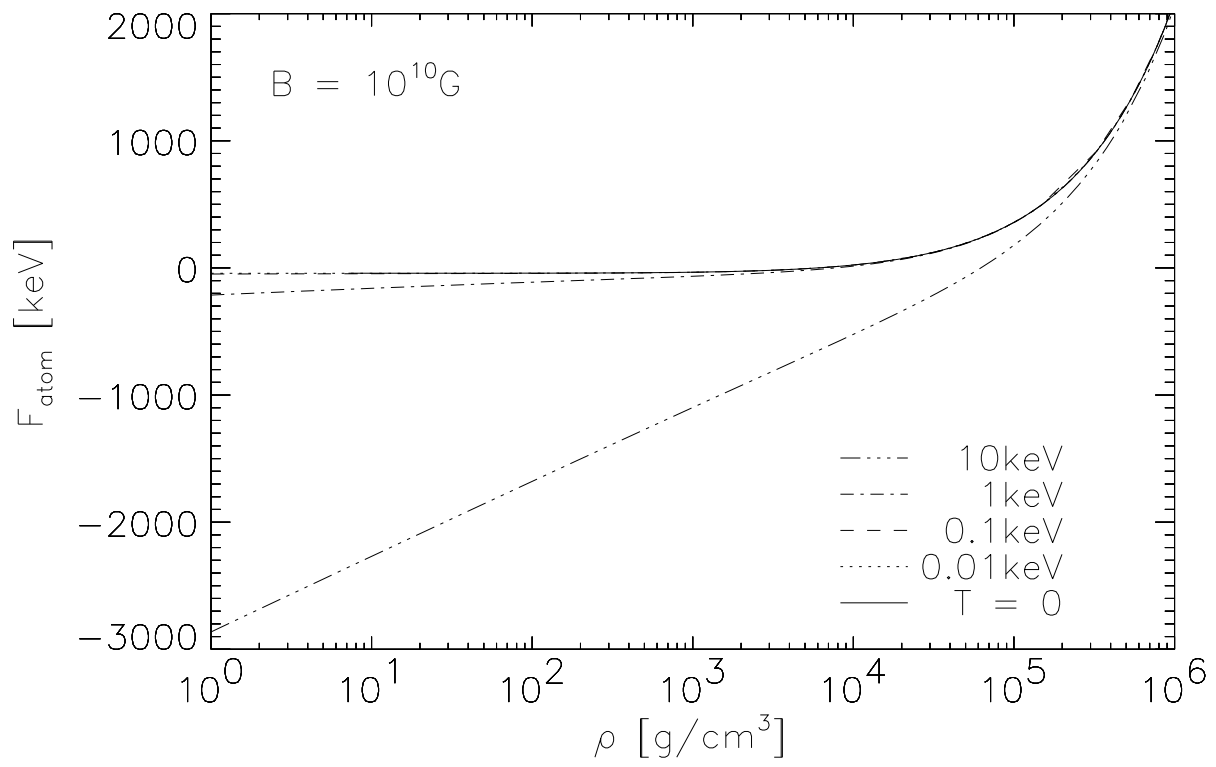


Fig. 7a.— The free energy of iron in bulk, F_{TF} , in the Thomas-Fermi approximation. Results are shown for several values of the temperature. (a) $B = 10^{10}$ G. (b) $B = 10^{12}$ G.

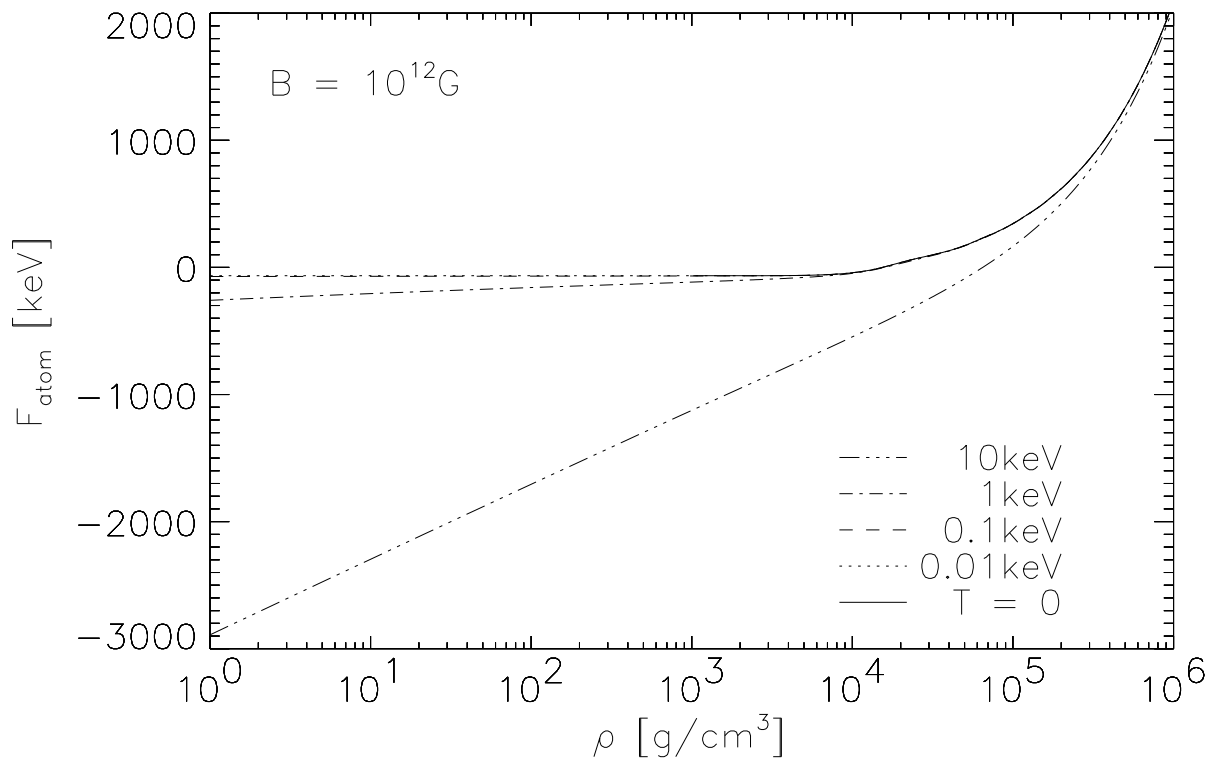


Fig. 7b.—

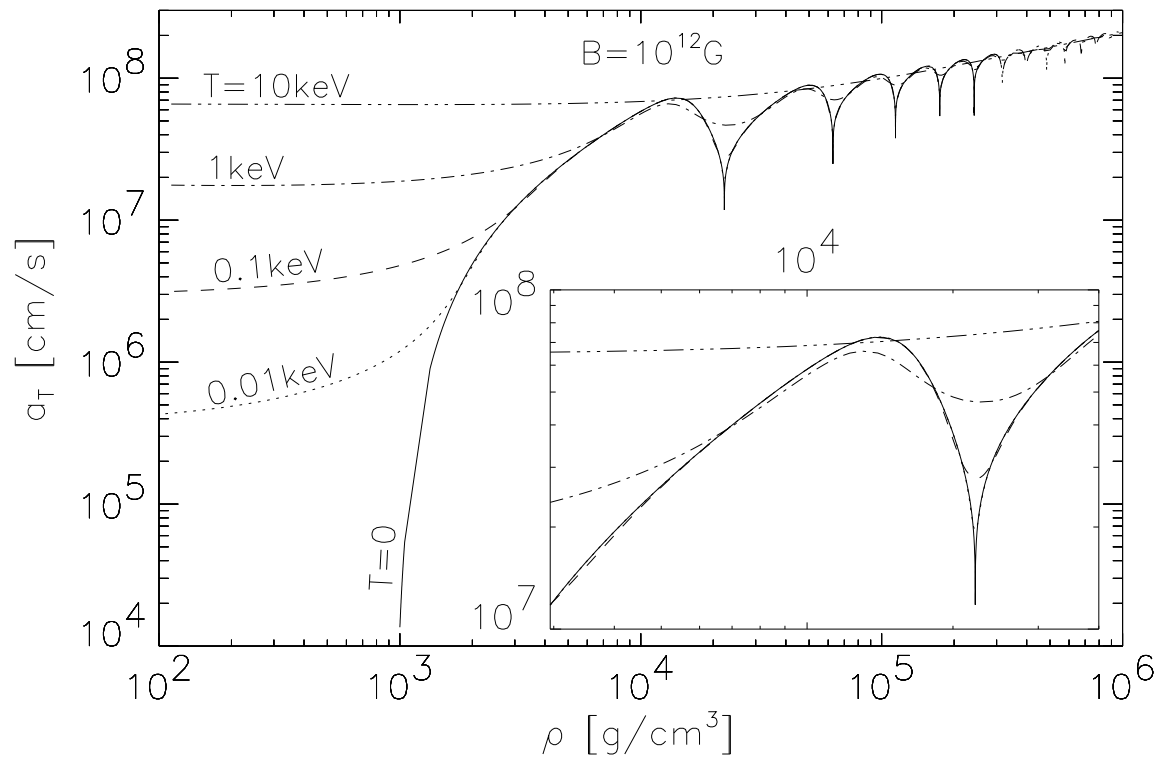


Fig. 8.— The isothermal sound velocity in bulk matter made of iron in the Thomas-Fermi approximation. Each curve corresponds to a given value of the temperature as indicated. The inset shows details around the peak of the first oscillation.

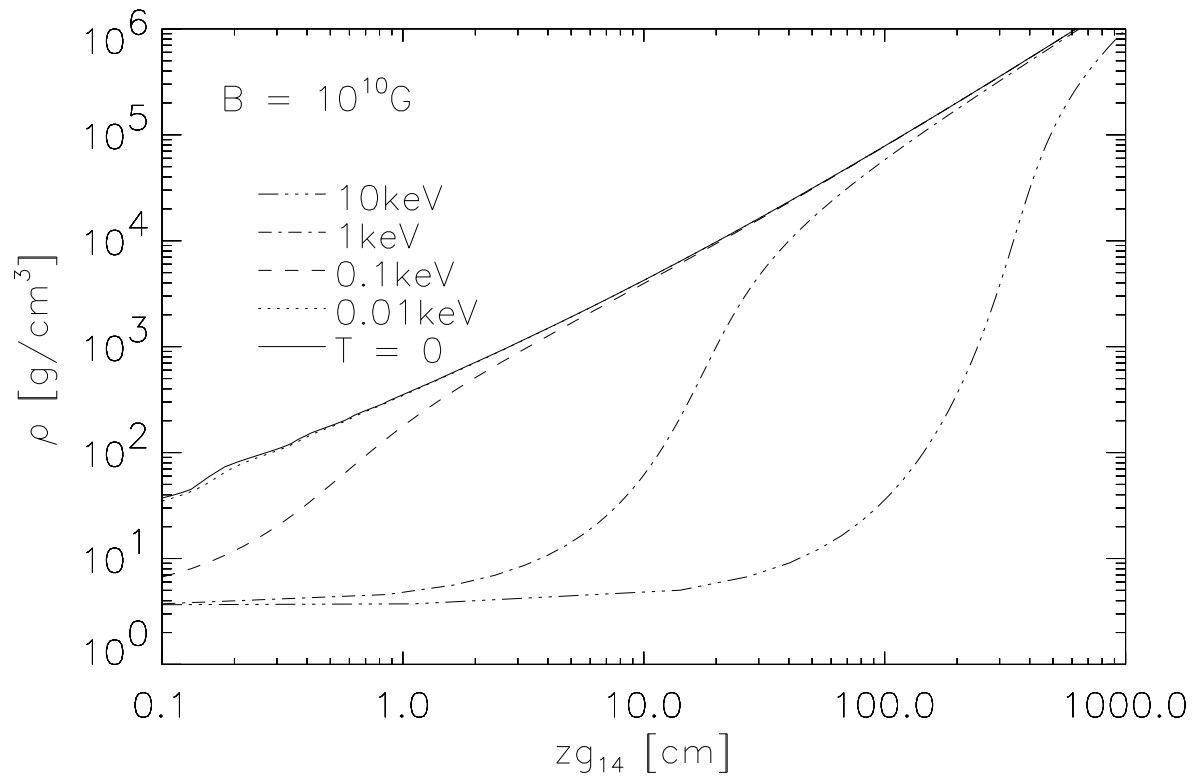


Fig. 9a.— The density of isothermal surface layers of neutron stars as a function of depth in the Thomas-Fermi approximation. Results are shown for five values of the temperature and two values of the magnetic field strength. The surface gravity is written in units of $10^{14} \text{ cm s}^{-2}$. Since isothermal atmospheres extend to infinity in the TF approximation the depth shown is measured from the point where the surface would be at zero temperature. (a) $B = 10^{10} \text{ G}$. (b) $B = 10^{12} \text{ G}$.

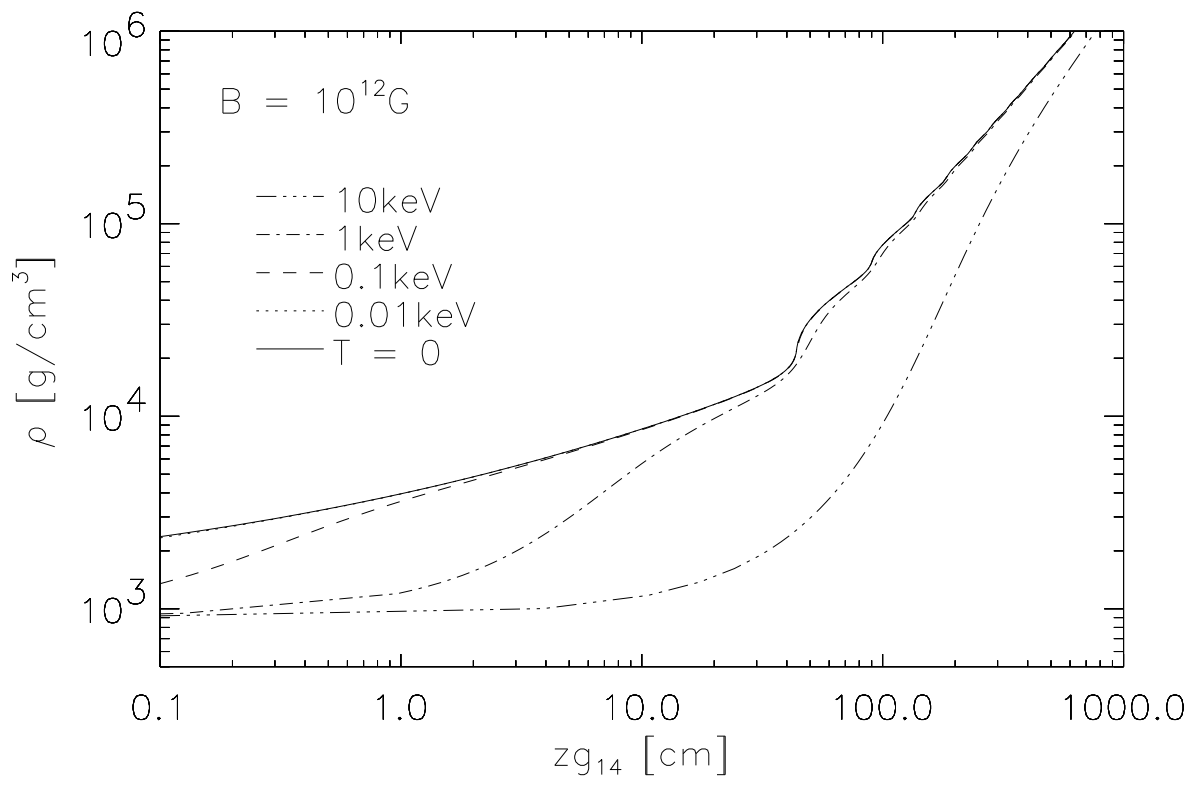


Fig. 9b.—

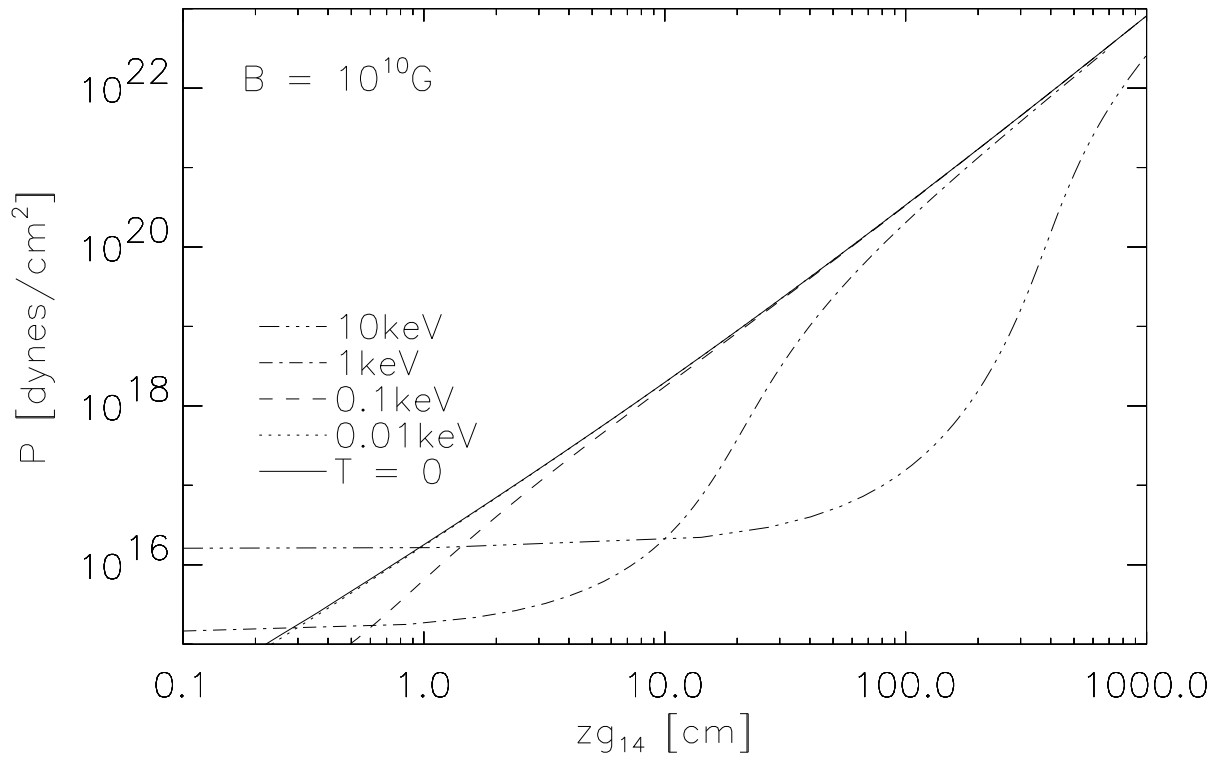


Fig. 10a.— The pressure of isothermal surface layers of neutron stars as a function of depth in the Thomas-Fermi approximation. Results are shown for five values of the temperature and two values of the magnetic field strength. See the text and the caption for figure 9a for further explanations. (a) $B = 10^{10}$ G. (b) $B = 10^{12}$ G.

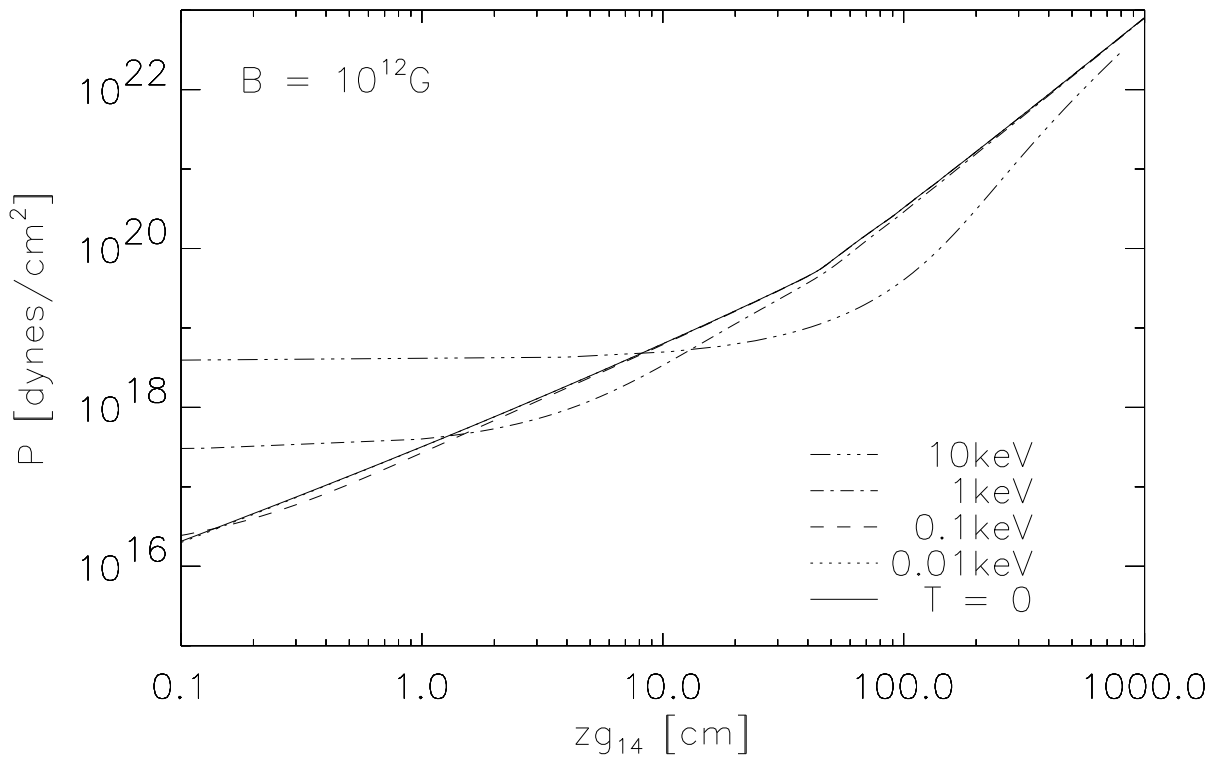


Fig. 10b.—